Haptic Modeling of Contact Formations and Compliant Motion

Jing Xiao, Qi Luo, Song You
Computer Science Department
University of North Carolina – Charlotte
Charlotte, NC 28223, USA
{xiao, qluo}@uncc.edu

Abstract

This paper models the effects of different contact formations and compliant motion on haptic rendering, taking into account friction and gravity. When a held rigid object interacts with another rigid object (in a task such as assembly), the force and moment felt by the operator at any instant depend not only on the contact region but also on the *type* of the contact state and the *type* of motion of the held object prior to reaching the current contact configuration, especially in the presence of friction and gravity. We address the modeling of such haptic effects by extending our study for the case of two interacting convex polyhedral rigid bodies [13] to the more general case of interacting non-convex polyhedral objects involving more complex contact formations and compliant motion.

1. Introduction

Certain applications of haptic interaction, such as virtual assembly, virtual prototyping, and teleoperation, require the simulated haptic force and moment to be physically accurate, which in turn requires physically accurate modeling of contact forces and moments [1].

However, in haptic rendering, contact forces and moments have to be computed in real time, and the external force and moment exerted to the virtually held object/tool at any time by the human operator is unknown and part of what needs to be modeled. The real-time requirement is made more stringent by the fact that the force/moment computation has to be on top of collision/contact detection, which usually takes a substantial amount of time. To be fast, current work on general haptic rendering is either focused on a single point contact model (e.g., [2])[1] or based on approximation models of contact [3, 4], which compromise physical accuracy. Existing work on task-specific rendering often considers limited and particular cases of contact (e.g, [5]). There is a lack of research on real-time physically accurate haptic rendering for general contact situations involving multiple contact regions and different kinds of compliant motions. The problem is challenging because it requires identifying the *exact* type of contact, which implies the correct geometric and physical constraints and dictates how the contact force distributes to produce a moment, as well as taking into account effects of friction and gravity, all in real time.

In this paper, we tackle the problem by presenting an efficient method to model and render haptic effects caused by arbitrary interaction or contact between two polyhedral rigid objects in real-time, taking into account friction and gravity. The key idea is to solve for the contact force and contact moment analytically based on real-time identification of the exact type of the current contact state, the type of motion of the "held" object prior to reaching the current contact configuration, as well as the current contact configuration.

We have applied our method and tested its efficiency in a haptic manipulation environment that we developed, where a human operator can "pick up" a virtual object via a PHANToM Desktop device, make arbitrary contact to another virtual object freely, and make arbitrary compliant motion or guarded motion. The haptic force and moment are calculated instantly by the method at the high rate of 2*k*Hz during the haptic interaction, where the force rendered is smooth and felt realistic.

2. Review: Principal Contacts and Contact Formations

We use the notion *principal contact*s (PC) [6] as contact primitives to describe a contact state. As defined in [6], a PC is in terms of a pair of contacting surface elements (i.e., edges, vertices, and faces) that are not the boundary elements of other contacting elements. The types of non-degenerate PCs are shown in Fig. 1. Each non-degenerate PC has a *contact plane* as determined by the face involved or the two edges of an edge-edge-cross type of PC.

Based on the contact region of the PCs, we can further classify the non-degenerate PCs into the following three categories:

Plane PC: face-face, where the contact happens at a planar region.

[1]Single point contact is also often assumed in haptic rendering involving deformable objects.

Line PC: edge-face and face-edge, where the contact happens on an edge.

Point PC: vertex-face, face-vertex, edge-edge-cross, where the contact happens at a point.

An arbitrary contact state between two polyhedral solids can be described by the set of the PCs formed, called a *contact formation* (CF) [6].

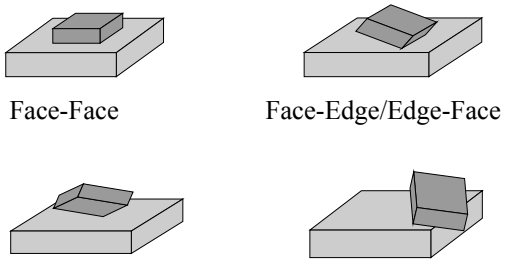

Fig. 1: Non-degenerate Principal Contacts

3. Basic Assumptions and Notations

We adopt the following assumptions and notations to model the haptic force and moment felt by a human operator when the "held" virtual object A (via a haptic device) interacts with a static virtual object B.

3.1. Basic Assumptions

Currently we limit our considerations to polyhedral solids (A and B) with evenly distributed mass so that the center of gravity is at the object's centroid p_c, whose coordinates can be simply calculated as the average coordinates of all the vertices of the object. We also assume that the objects have evenly distributed stiffness with a constant stiffness coefficient K. We use a Coulomb friction model with the static friction coefficient μ and kinetic friction coefficient μ_D.

We assume that the held object A can form a contact formation (CF) with the fixed object B with no more than three PCs that define different contact planes, since more than that often cause redundant PCs that can always be collapsed into fewer equivalent PCs [7]. We further assume that only one PC can be gained at a time, since the probability of gaining two PCs strictly simultaneously is extremely low in reality, although more than one PC can be broken at the same time.

3.2. Object and Task Frames, Force Representation of a CF

Let A also denote the object frame of A and B denote the frame of the fixed object B. Then the configuration of A at any instant is described by the homogeneous transformation matrix ${}^{B}\mathbf{T}_{A}$ from A to B.

When A and B are in a contact formation $CF=\{PC_1, \ldots PC_n\}$, we also establish a *PC-based task frame* according to each PC between A and B as the following: the origin of the frame is on the contact plane of the PC, the y-axis is along the normal of the contact plane pointing to the held object A, and the x- and z- axes are along the tangent of the contact plane and orthogonal to each other, following the right-hand rule (Fig. 2).

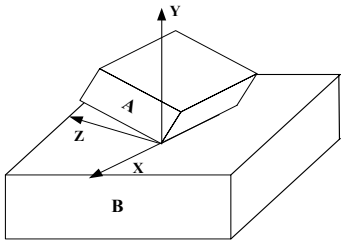

Fig. 2: An example task frame with respect to a line PC

We use the PC_j-based task frame to describe the contact force to A from B at PC_j, denoted as ${}^{j}\mathbf{F}_c$, j=1,…,n, which can be decomposed into a normal force along the $+y$ axis, ${}^{j}F_{cy}$, and a friction force ${}^{j}\mathbf{F}_{cf}$ along the xz plane (i.e., the contact plane) of the j-th task frame. With this notion, we can further define a *force representation* of CF as the set of contact forces excerted to A at the individual PCs of CF: $\{{}^{1}\mathbf{F}_c, \ldots, {}^{j}\mathbf{F}_c, \ldots, {}^{n}\mathbf{F}_c\}$, such that the total contact force to A from B at CF can be computed as: $\sum_j {}^{A}\mathbf{R}_j {}^{j}\mathbf{F}_c$, where ${}^{A}\mathbf{R}_j$ denotes the rotation transformation matrix from task frame j to the common object frame A.

4. Haptic Force Modeling

At any instant when the held A is contacting B, the haptic force felt by the human operator depends on the total contact force exerted to A by B, which in turn depends on not only A's configuration but also the current contact formation (CF) between A and B and the prior motion of A before reaching the current contact configuration. We will first describe how to identify the CF and the prior motion of A in real time to facilitate the modeling of contact force with physical accuracy as well as efficiency.

4.1. Real-time Identification of CFs

Real-time identification of CFs, especially those consisting of more than one PC, in the virtual world is a challenging task due to the ambiguity introduced by digital computation errors, which manifest to that for two surface elements a of A and b of B, concepts such as "a contacts b" (i.e., distance d_{ab}=0) or "$a \parallel b$" can only be approximated. For example, in Fig. 3, PC_1 could be identified as either one of the three possible types shown, and PC_2 could be identified as either of the

two possible types shown. If we consider just PC_1 (or PC_2) in isolation, then it does not matter which type the PC is identified because either one is a geometrically valid PC. However, here we have to consider both PC_1 and PC_2 together, and thus, if PC_1 is the edge-face PC, PC_2 has to be the vertex-face PC, for example, in order not to violate the geometric contact constraint. The combination of an edge-face PC_1 and a face-face PC_2, on the other hand, is not a valid CF. In general, the problem of identifying a multi-PC CF is how to find, among possible PCs, a right combination that forms a geometrically valid CF.

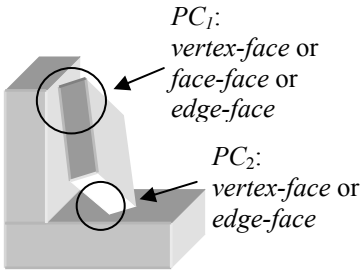

Fig. 3: Ambiguity in identification

Our approach is to first identify all possible PCs using the algorithm by Zhang and Xiao [8], which builds upon the efficient polytope distance algorithm by Gilbert et al. [9], and next from those PCs, find a combination of PCs that form a geometrically valid CF by looking up a table of valid CFs automatically built beforehand based on [10]. Note that among all possible sets of PCs, there is always at least one set that matches a valid CF. In our experiments, the time for search was almost negligible comparing to the time for collision detection, and real-time identification of CFs was achieved at the rate of 2 *k*Hz.

4.2. Prior Motion Types and Identification

Let t^- and t^+ indicate the times before and after A reaches the current contact configuration respectively. We call A's motion status during $[t^-, t^+]$ the motion of A prior to the current contact configuration, or the *prior motion*, which is of one of the following types:

MT1: guarded motion from no contact at t^- to a PC at t^+
MT2: no motion or compliant motion to maintain a CF
MT3: compliant motion to change some PCs in a CF
MT4: compliant motion to gain a new PC
MT5: compliant motion to break PCs

These prior motion types can be detected in real time based on:

(I) the change of A's configuration from t^- to t^+, which can be expressed by the homogeneous transformation matrix ${}^{-}\mathbf{T}_{+}$, consisting of a position vector ${}^{-}\mathbf{p}_{+}$ and a rotation matrix ${}^{-}\mathbf{R}_{+}$; and

(II) the current CF at t^+, $CF^+=\{PC_1, \ldots, PC_n\}$, $n \le 3$ (see Section 3.1), and the prior state of A at t^-, which could be either no contact or also a CF, CF^-.

The types and their detections are described below.

- Prior motion is **MT1** if A was not in contact at t^- (Fig. 4).

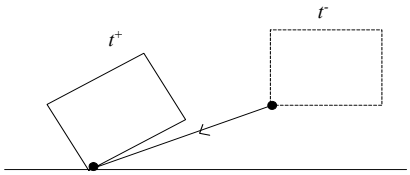

Fig. 4: An example of **MT1**

- Prior motion is **MT2** if $CF^+ = CF^-$ (Fig. 5).

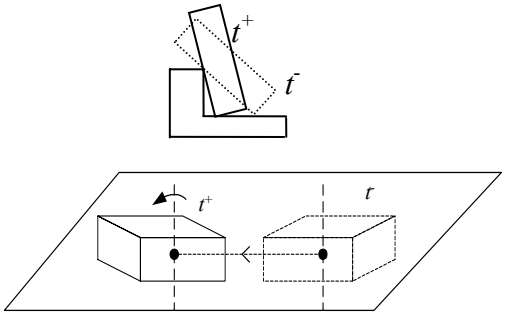

Fig. 5: Examples of **MT2**

- Prior motion is **MT3** if some PCs in CF^- are changed to their neighboring[2] PCs [10] so that $CF^+ \neq CF^-$, but CF^+ and CF^- have the same number of PCs (see Fig. 6 for examples).

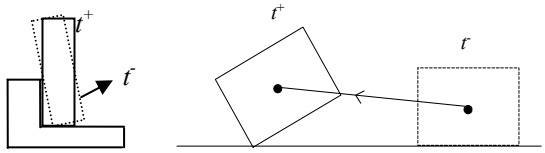

Fig. 6: Examples of **MT3**

- Prior motion is **MT4** if $CF^+=CF^- \cup \{PC_{\text{new}}\}$ (see Fig. 7 for examples).

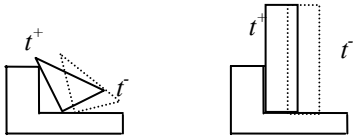

Fig. 7: Examples of **MT4**

[2] Note that since the motion is considered *instant*, it is not possible to change a PC to a non-neighboring PC.

- Prior motion is **MT5** if $CF^- \supset CF^+ \neq \varnothing$. Fig. 8 shows some examples.

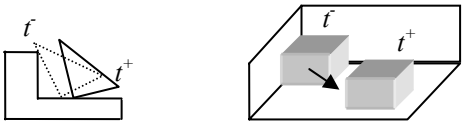

Fig. 8: Examples of **MT5**

4.3. Contact Normal Force at a Single PC

Recall that PC_j, j=1,…,n, of the current CF, CF^+, between A and B, describes a pair of *contacting* surface elements (Section 2), which means that the minimum distance d_j between the corresponding surface elements of PC_j is within a small threshold $\varepsilon > 0$ [11]. We model the magnitude of the contact normal force ${}^jF_{cy}$ based on the Hooke's law as:

$$ {}^jF_{cy} = K(\varepsilon - d_j) \tag{1}$$

where K is the stiffness coefficient. To prevent penetration, the constraint-based idea of a virtual proxy can also be used here [2].

4.4. Contact Friction Force

We now describe how to determine the contact friction forces $\{{}^1\mathbf{F}_{cf}, \ldots, {}^n\mathbf{F}_{cf}\}$ given ${}^-\mathbf{T}_+$ (which consists of ${}^-\mathbf{p}_+$ and ${}^-\mathbf{R}_+$), CF^+, CF^- (if it existed), and the type of prior motion.

Without losing generality, the friction force applied to A at each PC, PC_j, ${}^j\mathbf{F}_{cf}$, j=1,…,n, can be modeled as applied to the point p_j of A in the contact region corresponding to PC_j, which is the contact point if PC_j is a point PC, or the centroid of the contact region if PC_j is a line PC or a plane PC. Let ${}^j\mathbf{u}_{pj} = [a \;\; b \;\; c]^T$ be the unit vector denoting the direction of the linear velocity of p_j from t^- to t^+ represented in the task frame of PC_j. Let s_{pj} be the displacement of p_j from t^- to t^+ along the contact plane of PC_j. Both ${}^j\mathbf{u}_{pj}$ and s_{pj} can be obtained from the given information. As described in [13], for a single PC, there are two kinds of cases where the friction is static:

(**I**) Object A moved from no contact at t^- to forming PC_j at t^+, with, ${}^j\mathbf{u}_{pj}$ inside the static friction cone (Fig. 9). In this case the impulse force of collision dominates, and the static friction is

$$ {}^j\mathbf{F}_{cf} = [{}^jF_{cx} \;\; 0 \;\; {}^jF_{cz}]^T = {}^jF_{cy}[a/b \;\; 0 \;\; c/b]^T \tag{2}$$

(**II**) Object A maintained PC_j from t^- to t^+ and p_j hardly moved. In this case s_{pj} is sufficiently small so that

$$ s_{pj} \le \mu {}^jF_{cy}/K_p, \tag{3}$$

and the static friction can be computed as

$$ {}^j\mathbf{F}_{cf} = -K_p s_{pj} [a \;\; 0 \;\; c]^T \tag{4}$$

where K_p is the proportional control gain [2,11].

Other than the above cases, the friction at PC_j is dynamic:

$$ {}^j\mathbf{F}_{cf} = -\mu_D {}^jF_{cy}[a \;\; 0 \;\; c]^T \tag{5}$$

In general, if a CF^+ consists of more than one PC, we need to further take into account the effects of inter-PC geometric constraints in determining the friction forces $\{{}^1\mathbf{F}_{cf}, \ldots, {}^n\mathbf{F}_{cf}\}$. We now describe the process based on each prior motion status:

Prior motion is MT1:
Here CF^+ is a single-PC CF (see the related assumption in Section 3.1), and the friction is either determined by (2) (if ${}^j\mathbf{u}_{pj}$ is inside the static friction cone) or by (5).

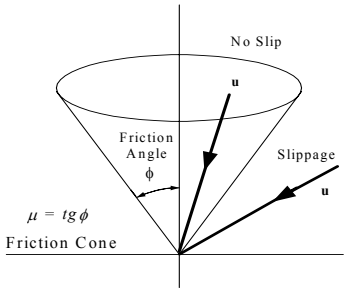

Fig. 9: Static Friction Cone

Prior motion status is MT2:
We need to further identify, given the CF is maintained, or $CF^+ = CF^- = CF$, whether ${}^-\mathbf{T}_+$ represents

(a) no actual physical motion,
(b) a motion that must involve translation, or
(c) a motion that can be a pure rotation about a contact edge or point.

There are two situations when (a) is true. First, if s_{pj} satisfies (3) for all j, j=1,…,n, then the friction at every PC is static, and (4) applies to every PC_j. Second, if ${}^-\mathbf{T}_+$, which captures how A is moved in the virtual space, does not correspond to a possible physical motion satisfying the contact constraints, then (a) is true. This is the case when the equivalent axis of rotation $\hat{\mathbf{u}}$ computed from ${}^-\mathbf{R}_+$ is not (approximately) along a possible axis of rotation to maintain CF [12] (see Fig. 10-i) or else ${}^-\mathbf{p}_+$ is not (approximately) along a possible translation axis to maintain CF (see Fig. 10-ii). In such a case, the friction applied to A at each PC_j needs to be static: (4) applies if s_{pj} satisfies (3); otherwise, ${}^j\mathbf{F}_{cf}$ is set to be the maximum static friction:

$$ {}^j\mathbf{F}_{cf} = -\mu {}^jF_{cy}[a \;\; 0 \;\; c]^T \tag{6}$$

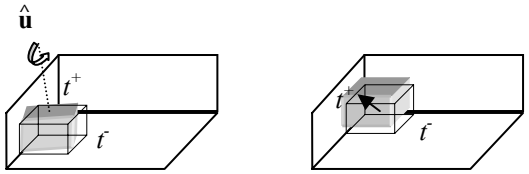

(i) (ii)

Fig. 10: Examples of no actual physical motion

Case (b) is true if (a) is not, and CF does not have a pure rotational degree of freedom [12], i.e., no pure rotation can maintain CF. In such a case, the friction applied to A at each PC_j needs to satisfy (5).

Case (c) is true if neither (a) or (b) is true. In such a case, if when $j=i$, $s_{pi} = \min_j s_{pj}$, and s_{pi} satisfies (3), a pure compliant rotation is indicated, and the friction at PC_i should be static and satisfies (4), while the friction at each PC_j, $j\neq i$, satisfies (5). Otherwise, the friction at every PC is dynamic and satisfies (5).

Prior motion is MT3:
Again we need to see if a pure compliant rotation is possible or not. If from CF^- to CF^+, the transition cannot be made by a pure rotation based on the CF types, the friction at each PC_j of CF^+ needs to satisfy (5). Otherwise, the friction forces can be determined as described in Case (c) of **MT2** above.

Prior motion is MT4:
If PC_k is the newly gained PC in CF^+, and ${}^k\mathbf{u}_{pk}$ is inside the static friction cone, then the friction force at PC_k is static and satisfies (2), and the friction force at each PC_j, $j\neq k$, should also be static, either satisfying (4), if s_{pj} satisfies (3), or else (6). Otherwise, the friction force at every PC of CF^+ should be dynamic and satisfy (5).

Prior motion is MT5:
Among all PC_j of CF^+, $j=1, 2\ldots$, if for PC_i, $s_{pi} = \min_j s_{pj}$, and s_{pi} satisfies (3), a pure compliant rotation MT5 is indicated, and the friction at PC_i should be static and satisfy (4), while the friction at each PC_j, $j\neq i$, satisfies (5). Otherwise, the friction at every PC is dynamic and satisfies (5).

With the contact force at each PC_j of CF^+ determined, the total contact force ${}^A\mathbf{F}_c$ (with respect to A's frame) is:

$$ {}^A\mathbf{F}_c = \sum_j {}^A\mathbf{R}_j {}^j\mathbf{F}_c \qquad (7)$$

4.5. Haptic Force

With the contact force $\mathbf{F}_c$ determined, the haptic force $\mathbf{F}_h$ that the human operator should feel can be readily obtained as the sum of the contact force and the gravity force: $\mathbf{F}_h = \mathbf{F}_c + \mathbf{F}_g$, and can be rendered accordingly. To enable a smooth and stable rendering, we make $F_{cy}(t^+) = F_{cy}(t)$ if the prior motion is compliant and the difference in virtual deformation is small enough and also perform force interpolation or shading [2, 3] to the general $\mathbf{F}_c$.

5. Haptic Moment

The haptic moment felt by the human operator at any instant equals to the combined moment created by the contact force upon A and the gravity of A. Such a moment depends on how the contact force is distributed (or the equivalent points of action), which in turn depends on the *type* of the contact state. In the following, we describe the haptic moment with respect to A's frame, denoted as ${}^A\mathbf{M}_h$.

Let ${}^A\mathbf{p}_j$ be the position vector of p_j (i.e., the point or equivalent point of action of contact force at PC_j) with respect to frame A. Let ${}^A\mathbf{p}_g$ denote the position vector of the centroid of A. Denote the moment generated by the contact force at PC_j to be ${}^A\mathbf{M}_j$, then

$$ {}^A\mathbf{M}_j = {}^A\mathbf{p}_j \times {}^A\mathbf{R}_j {}^j\mathbf{F}_c \qquad (8)$$

and

$$ {}^A\mathbf{M}_h = \sum_j {}^A\mathbf{M}_j + {}^A\mathbf{p}_g \times {}^A\mathbf{F}_g \qquad (9)$$

6. Implementation

We have developed a program for real-time haptic rendering based on the introduced haptic modeling method. We have further applied a PHANToM^{TM} Desktop device from SensAble Technologies (Fig. 11) to display the computed haptic force in real-time, which is connected to a personal computer with Intel Pentium III Processor 700MHZ and 256 MB system RAM.

Fig. 11: Haptic interaction via a PHANToM Desktop

Fig. 12a and 12b show some experimental examples, where A, the moveable object is the cube, and the static object B is the other, non-convex object. A world coordinate system is attached to B as shown. A user can "pick up" the object A by virtually attaching the PHANToM device to A and move A randomly to make arbitrary CFs with the static environment B and feel the haptic force with the rendering rate of near 2 kHz (on the rather slow computer). The CF types of these examples are also indicated, where f, e, and v denote face, edge, and vertex respectively.

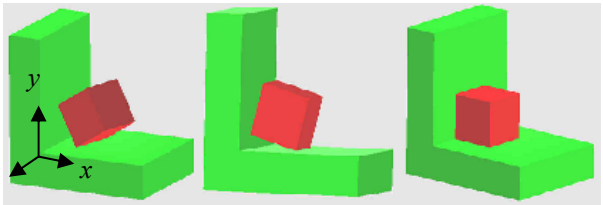

$\{e_A\text{-}f_B, v_A\text{-}f_B\}$ $\{e_A\text{-}f_B, e_A\text{-}f_B\}$ $\{f_A\text{-}f_B, f_A\text{-}f_B\}$

Fig. 12a: Some examples with an L-shaped B

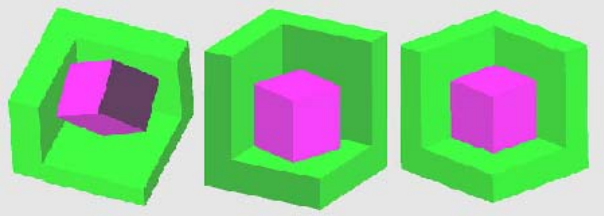

$\{v_A\text{-}f_B, v_A\text{-}f_B, v_A\text{-}f_B\}$ $\{e_A\text{-}f_B, e_A\text{-}f_B, f_A\text{-}f_B\}$ $\{f_A\text{-}f_B, f_A\text{-}f_B, f_A\text{-}f_B\}$

Fig. 12b: Some examples with a corner-shaped B

The following provides the values of the parameters used in our experiments, where m is the mass of A.

P	Value	P	Value
m	0.5 (kg)	K	2.3 (N/mm)
g	9.8 (N/kg)	K_p	1.6 (N/mm)
μ	0.7	ε	1.0 (mm)
μ_D	0.08		

Some simulated haptic forces/moments are shown below, with respect to the world coordinate system.

PC 1	PC 2	PC 3	Prior Move	**F** (N)	**M** (N*mm)
e-f	v-f		MT4	0.13945 -0.12271 -0.01508	-0.54008 -0.01996 1.68479
f-f	f-f	f-f	MT2.b	-0.01066 -0.22708 0.01135	-0.05858 -0.00135 -0.03085
e-f	e-f	f-f	MT2.a	0.00065 -0.40852 0.00119	-0.00481 -0.00007 0.00392
v-f	v-f	v-f	MT3	0.45949 -0.37587 0.32679	-1.78322 -0.18427 0.61172

7. Conclusions

We have introduced a novel approach to model the haptic force and moment felt by a human operator with respect to two interacting arbitrary polyhedral objects (of which one is held by the operator), taking into account friction and gravity. Our approach achieves efficiency and physical accuracy by taking advantage of real-time determination of contact formations and the knowledge of prior motion of the held object. Efficient and effective real-time identification of contact formations is made possible by searching a graph of valid CFs automatically built beforehand based on [13]. We are currently applying the strategy using a 6-D haptic device.

Acknowledgment

This work is funded by the U.S. National Science Foundation grant IIS-9700412.

References

[1] Hollerbach, J.M., "Some Current Issues in Haptics Research," *Proc. ICRA,* pp. 757-762, April 2000.

[2] Ruspini, D., Kolarov, K., Khatib, O., "Haptic Interaction in Virtual Environments," *Proc. of IROS*, Sept. 1997.

[3] Kim, Y., Otaduy, M., Lin, M.C., and Manocha, D., "Six Degree-of-Freedom Haptic Display Using Localized Contact Computations," *10th Symposium on Haptic Interfaces for Virtual Environment and Teleoperator Sys.,* March 2002.

[4] McNeely, W. et al., "Six degree-of-freedom haptic rendering using voxel sampling," *Proc. of ACM SIGGRAPH*, pp. 401-408, 1999.

[5] Maekawa, H., and Hollerbach, J. M., ``Haptic display for object grasping and manipulating in virtual environment," *Proc. ICRA*, pp. 2566-2573, May 1998.

[6] Xiao, J., "Automatic Determination of Topological Contacts in the Presence of Sensing Uncertainties," *Proc. of ICRA*, pp. 65-70, May 1993.

[7] Xiao, J. and Zhang, L., "Contact Constraint Analysis and Determination of Geometrically Valid Contact Formations from Possible Contact Primitives," *IEEE Trans. on Robotics and Automation*, 13(3):456--466, June 1997.

[8] Zhang, L. and Xiao, J., "Derivation of Contact States from Geometric Models of Objects," *Proc. IEEE Int. Conf. Assembly and Task Planning*, pp. 375-380, Aug. 1995.

[9] Gilbert, E., Johnson, D. Keerthi, S., "A Fast Procedure for Computing the Distance between Complex Objects in Three-dimensional Space," *IEEE J. of Robotics and Automation,* 4(2): 193-203*,* April 1988.

[10] Xiao, J., Ji, X., "On Automatic Generation of High-level Contact State Space," *Int. J. of Robotics Res.*, (& its 1st multi-media extension issue), 20(7):584-606, July 2001.

[11] Salcudean, S.E., Vlaar, T.D., "On the Emulation of Stiff Walls and Static Friction with a Magnetically Levitated Input/Output Device," *ASME Haptic Interfaces for Virtual Env. & Teleoperator Sys., Dynamic Sys. & Control*, pp. 123-130, April 1995.

[12] Ji, X. and Xiao, J., "Planning Motion Compliant to Complex Contact States," *Int. J. of Robotics Res.*, 20(6):446-465, June 2001.

[13] Xiao, J. and You, S., "Haptic Modeling Based on Contact and Motion Types," *Proc. of IROS2002*, pp. 2925-2930, Sept. 2002.